

# Learning to Learn in the Context of Spiking Neural Networks

Moritz Zanger - supervised by J. Camilo Vasquez Tieck<sup>1</sup>

**Abstract—L2L abstract - I will write it in the end**

## I. INTRODUCTION

Introduction to the topic

## II. RECURRENT NEURAL NETWORKS (RNNs)

Artificial Neural Networks (ANNs) are networks of biologically inspired computational units, neurons, that learn according to certain learning rules thus improving their ability to perform a desired task, often classification or regression problems. Accordingly, the performance demonstrated by ANNs is based on knowledge, inferred from data [58]. Many of the data driven problems in engineering involve the recognition of time dependent patterns (e.g. speech recognition, machine translation, machine vision in real-time video material), requiring special network architectures such as the Time-Delay Neural Networks (TDNN) [62] or Recurrent Neural Networks (RNNs). The latter revolve around the basic idea of including a loop in the networks neurons, allowing information to be passed from past steps of the networks state to the next.

### A. Training RNNs

Unfolding an RNN over time results in a more approachable representation of this model as seen in fig. x. Training a model of this structure can now be achieved in a similar way to the well-known backpropagation algorithm with the additional ability to encode longer past information [65].

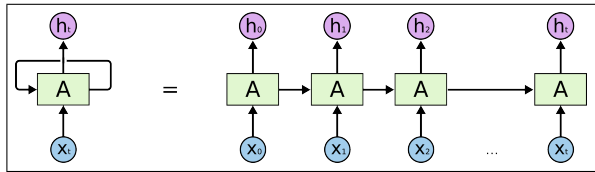


Fig. 1. Unrolled RNN [2]

The notation of symbols in the following is according to Jian Guo [30]. The inputs are denoted by vector  $\mathbf{x}$ , with components indexed by  $i$ . We similarly define the current hidden layer state as vector  $\mathbf{s}$ , components indexed by  $j$ , the previous hidden layer state as vector  $\mathbf{s}(t-1)$ , components indexed by  $h$ , the output layer as vector  $\mathbf{y}$ , components indexed by  $k$ . The weight matrices are written as bold uppercase Letters, where  $\mathbf{V}$  maps  $\mathbf{x}$  to the current state  $\mathbf{s}(t)$ ,  $\mathbf{U}$  maps the previous hidden state  $\mathbf{s}(t-1)$ , and  $\mathbf{W}$  transforms the current state  $\mathbf{s}(t)$  to the output layer  $\mathbf{y}$ . For

clearness, the previously defined symbols can be seen in fig. x. Furthermore we describe the relation between outputs and net input function  $net_j$  or  $net_k$  of a layer as the activation functions  $f(net_j(t))$  and  $g(net_k(t))$  respectively for the hidden and output layer. Including biases  $b_j$ ,  $b_k$  for the net input functions, we conclude that the hidden state becomes (1) and the output is described by (3).

$$s_j(t) = f(net_j(t)) \quad (1)$$

$$net_j(t) = \sum_i^l x_i(t)v_{ji} + \sum_h^m s_h(t-1)u_{jh} + b_j \quad (2)$$

$$y_k(t) = g(net_k(t)) \quad (3)$$

$$net_k(t) = \sum_j^m s_j(t)w_{kj} + b_k \quad (4)$$

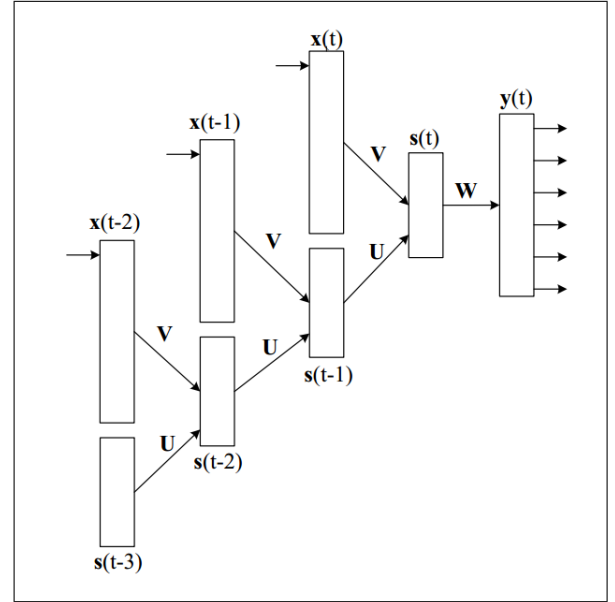


Fig. 2. An Unrolled RNN with shared weight Matrices  $\mathbf{U}$  and  $\mathbf{V}$  between temporal states [30]

In order to minimize the loss of our network, we define the widely used summed squared error (5) as a loss function with desired outputs  $d$ , total number of training samples  $n$  and the number of output units  $o$ . For computational reasons, the stochastic version of gradient descent utilizes only subsets of our training collection, up to the extremum where  $p = n$ .

$$E = \frac{1}{2} \sum_p^n \sum_k^o (d_{pk} - y_{pk})^2 \quad (5)$$

<sup>\*</sup>This work was not supported by any organization

<sup>1</sup>Moritz Zanger, Faculty of Mechanical Engineering, Karlsruhe Institute of Technology zanger.moritz@googlemail.com

By propagating this error backwards throughout the network, we can construct the loss functions derivative with respect to each weight in order to obtain the weight update of a specific weight for the next timestep. Applying the chain rule, the weight updates for connections between hidden and output layer  $\Delta w_{kj}$  are denoted in (6) and for connections between input and hidden layer  $\Delta w_{ji}$  in (7):

$$\Delta w_{kj} = \eta \sum_p \delta_{pk} s_{pj} = \eta \sum_p (d_{pk} - y_{pk}) g'(net_{pk}) s_{pj} \quad (6)$$

$$\Delta w_{ji} = \eta \sum_p \delta_{pj} x_{pi} = \eta \sum_p \sum_k \delta_{pk} w_{kj} f'(net_{pj}) x_{pi} \quad (7)$$

The terms  $\delta_{pk}$  and  $\delta_{pj}$  are referred to as the components of the specific error vectors per layer. The netfunction of our hidden layer  $net_{pj}$  however still depends on the previous state  $s_{t-1}$  which in turn depends on previous states itself. Unfolding the network up to a temporal depth  $\tau$  with the same weights throughout the timesteps (fig.x) allows us to define an error vector for previous time steps as seen in (8).

$$\delta_{pj}(t-1) = \sum_h \delta_{ph}(t) u_{hj} f'(s_{pj}(t-1)) \quad (8)$$

More detailed reflections on the construction of the above equations can be found in [30]. The procedure previously used to obtain  $\delta_{pj}(t-1)$  allows for theoretically arbitrary depths  $\tau$  to be recursively calculated. In practice, large values for  $\tau$  and the subsequently generated long-term dependencies tend to be difficult to handle with gradient descent. This is due to the fact, that deriving error terms through multiple layers of an unfolded RNN de- or increases the magnitude of the resulting derivative exponentially, thus creating phenomena known as vanishing and exploding gradient.

@draft Because the parameters are shared by all time steps in the network, the gradient at each output depends not only on the calculations of the current time step, but also the previous time steps. This is called Backpropagation Through Time (BPTT) vanilla RNNs trained with BPTT have difficulties learning long-term dependencies (e.g. dependencies between steps that are far apart) due to what is called the vanishing/exploding gradient problem. There exists some machinery to deal with these problems, and certain types of RNNs (like LSTMs) were specifically designed to get around them.

### B. Long Short Term Memory (LSTM)

The previously described problems occurring when facing long term dependencies in RNNs are successfully tackled by the Long Short Term Memory (LSTM), first introduced by Hochreiter and Schmidhuber [33]. As shown by Hochreiter, a key idea towards avoiding the explosion or vanishing of gradients through a large number of timesteps is to enforce a constant errorflow through a single unit  $j$  by requiring the

net activation derivative of  $j$  to follow equation 9 with weight  $w_{jj}$  of a single connection to itself.

$$f'_j(net_j(t)) w_{jj} = 1.0 \quad (9)$$

Simple integration over time gives us  $f_j(net_j(t)) = \frac{net_j}{w_{jj}}$ , a linear function. Therefore our recurrent definition of  $net_j(t+1) = w_{jj} y^j(t)$  leads us to the conclusion 10, that the unit  $j$ 's activation has to remain constant [33]:

$$y_j(t+1) = f_j(net(t+1)) = f_j(w_{jj} y^j(t)) = y^j(t) \quad (10)$$

This approach alone however leads to a problem that becomes evident during learning in networks with more than one neuron connected to the so far single unit  $j$ . The input weights  $w_{ji}$  from neuron  $i$  and the outgoing weights  $w_{kj}$  to neuron  $k$  now are both responsible for regulating the desired protection from yet unneeded information of previous timesteps as well as conceiving said information when deemed necessary. Take for instance a language processing network trying to estimate the importance of a recently heard subject "You", regarding the following words "are a tall, friendly, level-headed, smart person". The same weights that have just been trained on this sentence would receive very conflicting weight updates in the next learning step, when confronted with the new sentence "You are a person".

To overcome this shortcoming, Hochreiter and Schmidhuber propose a more context sensitive approach, using separate gates for forgetting, input and output regulation within a single cell, as seen in fig. x.

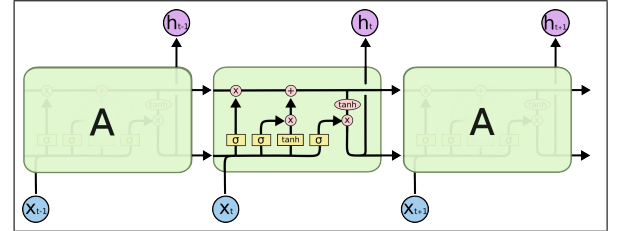


Fig. 3. (has to be edited) Inner composition of an LSTM cell (co-lah.github.io)

The *forgetgate* consists of a sigmoid-activated layer  $f_t$ , essentially determining, how much of the previous output  $h_{t-1}$  should be kept within the LSTM Cell State  $C_t$ , based on its own set of weights  $W_f$  and biases  $b_f$ :

$$f_t = \sigma(W_f \times [h_{t-1}, x_t] + b_f) \quad (11)$$

The *inputgate* is composed of the sigmoid-activated layer  $i_t$  and the hyperbolic-tangent-activated layer  $\tilde{C}_t$ , creating candidates for replacing the current (possibly forgotten) cell state  $C_{t-1}$  with  $i_t \times \tilde{C}_t$ . Each of these layers, again, have their own set of weights and biases  $W_i$ ,  $b_i$ ,  $W_c$  and  $b_c$ , leaving us with the respective layer outputs (12) and (13) [2]:

$$i_t = \sigma(W_i \times [h_{t-1}, x_t] + b_i) \quad (12)$$

$$\tilde{C}_t = \tanh(W_c \times [h_{t-1}, x_t] + b_c) \quad (13)$$

In order to determine whether to inhibit possibly disturbing signals to following cell states, the output  $h_t$  is filtered

by applying  $\tanh(x)$  and multiplying with the outcome of the  $outputgatelayer_o_t$  with weights  $W_o$  and biases  $b_o$  and results in the total output  $h_t$ :

$$o_t = \sigma(W_o[h_{t-1}, x_t] + b_o) \quad (14)$$

$$h_t = o_t \times \tanh(C_t) = o_t \times \tanh(f_t \times C_{t-1} + i_t \times \tilde{C}_t) \quad (15)$$

This design allows for separate read and write capabilities and therefore enables capture of error signals within the cell for longer periods of time than previously possible with standard RNNs [33]. Many applications with record-breaking performances followed, thus proving the state-of-the-art standing of LSTMs in temporal problems. Graves and Jaitly [27] provide an overview over variations of the vanilla LSTM, such as the introduction of peepholes by Gers and Schmidhuber [24] or the lighter Gated Recurrent Unit (GRU) by Cho et al. [14]. Furthermore, attention-based models as proposed by Graves et al. [28], Graves et al. [26] and Nee-lakantan et al. [49] are promising more recent developments in the field of RNNs.

### III. SPIKING NEURAL NETWORKS (SNN)

The above described ANN models differ from Feedforward Networks in regards of activation, connection design, learning rules and more, yet implicitly share a common-ground in how they encode information in their neurons. These second generation neural networks, as commonly described in the literature, activate on continuous functions and make use of their derivability in backpropagation. Maass et al. [41] provide a setup that integrates a different, biologically more accurate take on modelling neuron activation. These Spiking Neural Networks (SNN) employ integrate-and-fire neurons [40] which encode information with an additional temporal factor in its activation pulses, increasing the density of encoded information.

#### A. Neurons - Activation and Signal Processing

The fundamental idea behind the computational units of an SNN builds on integrating a temporal factor in the representation of information. Various models of these spiking neurons, such as the integrate-and-fire model [4], the Hodgkin-Huxley model [34], the model by Izhikevich [35] and the Spike Response Model by Gerstner [25] exist and vary in their attempt to trade off biological accuracy and computational complexity [29]. The Leaky-Integrate-and-Fire model is nowadays the most widespread approach due to its simplicity and computational advantages. The representation of the activation process of the neuron is modeled by an electrical circuit in which the membrane potential, threshold voltage, resting potential and leak rate are realized through a capacitor, gate, battery and resistance respectively [4][54] (maybe fig. Ponulak).

#### B. Spike-based Neural Codes

Whilst encoding and decoding of the desired information is much simpler and intuitive in second generation neural network models, this is a larger challenge for the time-dependent neurons in an SNN, due to the arbitrary number

of theoretically possible ways of encoding information in the neurons. In fact the biological process of information decoding is still being researched, whereas various methods have been introduced in Neuroscience Engineering.

- Rate Coding is an approach aiming at recording spike rates during fixed time frames. This implementation of spike encoding can be seen as an analog way of interpreting spike trains in SNNs.
- Latency Coding encodes spikes based on their timing rather than their multiplicity. This encoding has for example been used in unsupervised learning, and supervised learning methods like SpikeProp [10]
- Fully temporal codes are a more general term which includes the above mentioned approaches. It encodes information based on the precise timing of each spike in a spike train [29]
- Gaussian Coding applies a gaussian distribution over recorded spikes of each neuron and encodes information based on their stochastic occurrence.

#### C. Learning in Spiking Neural Networks - Synaptic Plasticity

While conventional neural networks employ a stochastic version of gradient descent to backpropagate errors throughout the network, the same approach is difficult to apply in the realm of SNNs due to their temporal dependence and the non-differentiability of spike trains. Whereas multiple learning rules addressing SNNs exist (such as Hebbian Rule, Binarization of ANNs, Conversion from ANNs and Variations of backpropagation [53], a state-of-the-art algorithm such as backpropagation has yet to emerge. We will first focus on a more biologically motivated training rule called spike-timing-dependant plasticity (STDP). The key feature of this approach is to adjust weights between a pre- and post-synaptic neuron according to their relative spike times within an interval of roughly tens of milliseconds in length [10]. If a postsynaptic neuron fires shortly after its presynaptic neuron, the connecting weights is strengthened whereas presynaptic neurons firing after the postsynaptic neuron will lead to weakening of the weights. The experimentally refined and commonly used formula according to Dan et al. [16] for the exact weight updates is given in (16)

$$\Delta w = \begin{cases} Ae^{-\frac{-(t_{pre} - t_{post})}{\tau}} & t_{pre} - t_{post} \leq 0, A > 0 \\ Be^{-\frac{-(t_{pre} - t_{post})}{\tau}} & t_{pre} - t_{post} > 0, B < 0 \end{cases} \quad (16)$$

where  $\delta w$  is the update of the weight  $w$  with adjustable learning rates  $A, B$  and pre/postsynaptic fire times  $t_{pre}/t_{post}$ . A related rule to STDP is the more general Hebbian learning rule, which in contrast to STDP claims, that synaptic efficiency arises from the general temporal proximity of these signals independent from the order of occurrence. This rule is often referred to as "fire-together-wire-together". Both mentioned approaches are illustrated in Fig. x

The above mentioned learning rules share the common characteristic in which they don't require information other than what is available in a local neighborhood of neurons.

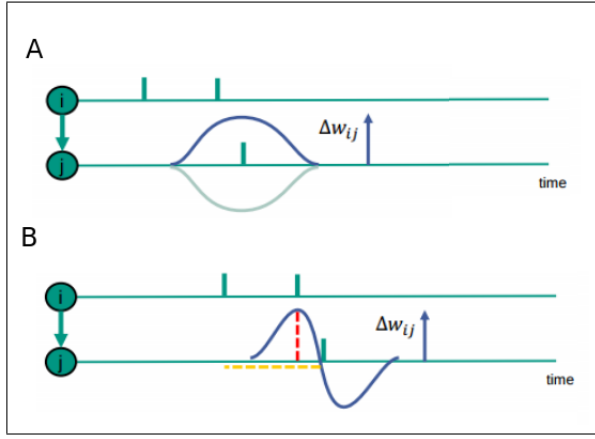


Fig. 4. **A:** illustration of weight-updates  $\Delta w_{ij}$  with presynaptic neuron  $i$  and postsynaptic neuron  $j$  according to STDP  
**B:** symmetric hebbian learning rule with weight update  $\Delta w_{ij}$ , presynaptic neuron  $i$  and postsynaptic neuron  $j$

Therefore they do not require the biologically unrealistic transport of weight information throughout numerous layers of neurons [56] [13] [15][18]. Consequently, these learning rules are suited for unsupervised learning tasks and pose interesting insights from a neuroscientific standpoint. Guyonnet et al. [45] [61] showed, that STDP-equipped SNNs are capable of learning input patterns and decrease latencies between in- and output throughout training. Furthermore, T. Masquelier [45] and S. R. Kheradpisheh [61] point out, that the increased density of encoded information in SNNs allows even a single neuron to learn spatio-temporal patterns. However practical usability of these learning rules raises the need for proper supervised learning algorithms, often clashing with mathematical feasibility, numerical efficiency or biological plausibility. In this, we encounter problems, such as the non differentiability of spikes and the biological absence of outer error signals in deeper layers. These challenges remain generally unsolved, however various promising advances have been proposed in tackling them. In a rather biological aspect, Markov et al.[44] propose the existence of feedback connections, designed to project information within hierarchically organized networks. Approaches such as SpikeProp by Bohte and Kok deal with discontinuous nature of spiking neurons by linearizing the relationship between post-synaptic input and the resulting spiking time, consequently circumventing the discontinuity of the thresholding function [10]. Further techniques aiming at surrogating the gradient of discontinuous activations have been researched and tested by Neftci et al. [50].

#### D. Eligibility Traces

When performing on tasks that last between few seconds to multiple minutes until an output of an ANN can be evaluated, it can be difficult to assign blame or reward for the achieved outcome to particular spikes which usually happen within the range of few milliseconds. Accordingly, the field of reinforcement learning and neuroscience provide an approach to close this temporal gap by introducing a

dynamic variable in synapses henceforth called eligibility trace [59]. Eligibility traces record recent synaptic activity and enable better assignment of error signals to culprit neurons. Neuroscience suggests, that eligibility traces may be a key feature to neuromodulatory reward based learning such as the midbrain dopaminergic system [52]. Updates to the eligibility trace are described by the eligibility function  $f_c(t)$  in close accordance to STDP spike patterns of pre-/postsynaptic and post-/presynaptic spike pairs. Respectively, a pair of spikes will increase or decrease the eligibility trace  $c_{ji}(t)$  of the synapse over time (fig. x A). Reward signals  $d(t)$  received after a time delay can now be assigned to synapses using a learning rule that changes synaptic weights proportionally to the product of  $c_{ji}(t)$  and  $d(t)$ , (17).

$$\frac{d}{dt} w_{ji}(t) = c_{ji}(t) d(t) \quad (17)$$

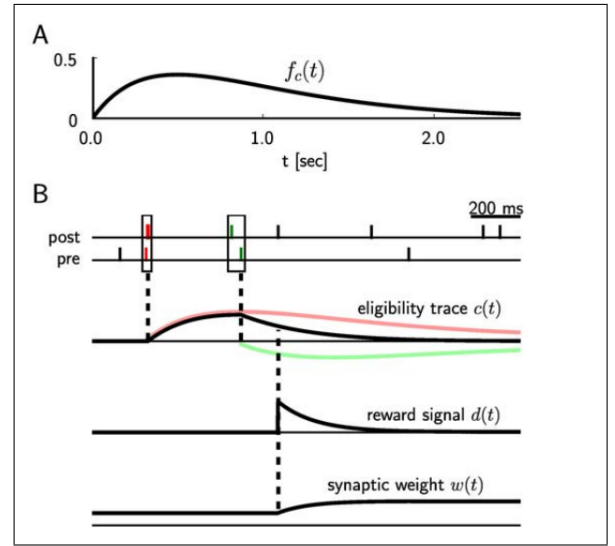


Fig. 5. **A:** Eligibility function  $f_c(t)$ . Illustrated are values for a pre-/postsynaptic spike pattern. Negative for post-/presynaptic spike patterns.  
**B:** Contributions of spike patterns (red and green) to an eligibility trace  $c(t)$  and the according weight update  $w(t)$  upon reception of a reward  $d(t)$ . [39]

#### IV. LEARNING TO LEARN (L2L)

The field of reinforcement learning (RL) has recently celebrated great success at reaching human-like and even surpassing human abilities on complex environments such as Atari [47] and Go [60] with the implementation of Deep Neural Networks to account for non-linear function approximation over high-dimensional action and state spaces. However Artificial Intelligence in general [38] and Reinforcement Learning in particular [22] currently suffer from two major drawbacks, that are limiting their application and design [64]:

- Firstly the immense volume of required training data and the relatively expensive generation of this data in often simulated environments.
- Secondly RL-algorithms often have to be heavily tailored to a specific range of tasks and various algorithms,

each of which depending on numerous hyperparameters and thus requiring immense efforts compared to currently reached results.

Botvinick et al. [12] explain these weak spots in AI with a need for low learning rates and the bias-variance trade-off. Low learning rates are necessary to prevent both catastrophic interference (discarding previously reached successful configurations) and overfitting [31]. The bias-variance trade-off is a phenomenon describing the contrary working directions of efficiency-driving biases or priors and performing on a wider range of tasks.

With some approaches addressing these issues existing, Landsell and Kording[38] argue, that these L2L approaches can be categorized into either Learning to Optimize or Structure Learning. Learning to Optimize focusses on the general adaption of network parameters to achieve efficient learning rules on arbitrary Task classes without hand-selection. Similarly to the way gradient descent applies small changes of the weights in an NN in order to minimize loss functions, the design of AI systems can be viewed as an optimization problem itself, that requires parameter optimization to ensure a well performing algorithm. Structure Learning on the other hand makes use of structural similarities within a finite family of tasks to reach higher data efficiency due to its prior adaptiveness to the given family of tasks [38].

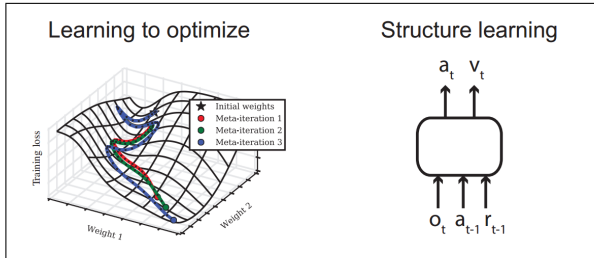


Fig. 6. Types of learning-to-learn in AI. Learning-to-learn can be roughly divided into learning to optimize and structure learning. In AI, hyperparameter optimization is an example of learning to optimize [42], while a recurrent neural network taking rewards, actions and observations can often be used to perform structure learning [64] [38].

#### A. Learning to Reinforcement Learn (meta-RL) and RL

A high level architecture consisting of a learner (performing on the task itself) and a meta-learner (adjusting the learner) is inherent to most implementations of L2L [38] and has been refined in various ways to create new L2L Systems, as will be explained in the following section.

Wang et al.[64] as well as Duan et al.[22] introduced frameworks that can be thought of as generating an RL algorithm of their own and provide agents, who are given a predesigned prior to efficiently learn any task  $T \in \mathcal{F}$  (in the original papers denoted as a Markov Decision Process (MDP)  $m \in \mathcal{M}$ ) from a family of interrelated tasks  $\mathcal{F}$  (i.e. a set of MDPs  $\mathcal{M}$ ).

In their attempt to design an algorithm, capable of performing well on a set  $\mathcal{M}$  of Markov Decision Processes (MDPs), Duan et al. implement a nested system in which learning an RL algorithm is regarded as a reinforcement learning problem itself, hence the name RL [22]. The agent performing on a randomly drawn separate MDP  $m \in \mathcal{M}$  from the distribution  $\rho_{\mathcal{M}} : \mathcal{M} \rightarrow R_+$  is represented as a recurrent neural network (RNN) which outputs the probability distribution over the tasks action-space  $\pi$  (policy) based on a function  $\phi(s, a, r, d)$  of the tuple (state, action, reward, termination flag) (Duan et al.). On a higher abstraction layer, this RNN is being optimized by an implementation of Trust Region Policy Optimization (TRPO), a state-of-the-art DRL algorithm [57] with several advantages regarding stability and hyperparameter dependance.

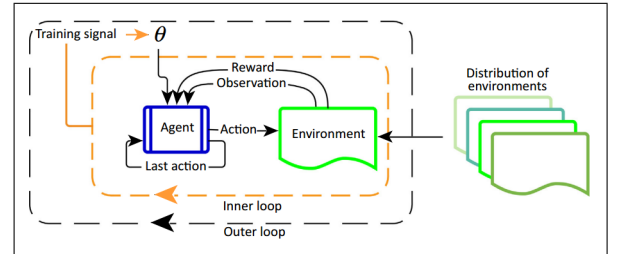


Fig. 7. Schematic of Meta-reinforcement Learning, Illustrating the Inner and Outer Loops of Training. The outer loop trains the parameter weights  $\theta$ , which determine the inner-loop learner (Agent, instantiated by a recurrent neural network) that interacts with an environment for the duration of the episode. For every cycle of the outer loop, a new environment is sampled from a distribution of environments, which share some common structure [12].

Wang et al.[64] define a similar setup in which a RL-algorithm is responsible for learning the weights of a nested RNN. Both, inner and outer loop in this framework draw their learning experience from the reward information generated by the actions of the RNN, where the RNN holds information on the previously chosen action and the subsequent rewards. However the process of learning in each of these loops is realized differently and results in specializations of different scopes. While the wrapping RL-algorithm used to optimize the weights of the RNN operates over the entire set of episodes, that is to say all MDPs  $\mathcal{M}$ , learning of the nested RNN within a single task  $m$  is based on the inner recurrent dynamics of the network. Notably, the RNN is able to encode learned experience on a specific task using only its inner memory variables, leaving us with the observation that a well working short-term memory is a key factor to learning on different levels of abstraction. The policy outputs  $\pi$  of this network can then be viewed as an RL-algorithm on its own, resulting in the name meta-RL. For the implementation of this framework Wang et al. [64] used an LSTM according to Hochreiter and Schmidhuber [33] to account for the inner RNN, while both synchronous asynchronous advantage actor critics (A2C and A3C) (Mnih et al.) were employed to learn inter-cell weights. The



observation vectors of experiment environments were either directly fed to the LSTM one-hot-encoded or passed through an additional deep encoder model[64]. Experiments on a series of bandit problem and two MDP-centered problems with implementation architectures as described above showed, that meta-RL delivers competitive results compared to problem-specific algorithms (Thompson sampling, UCB, Gittins) while operating on a wider set of tasks.

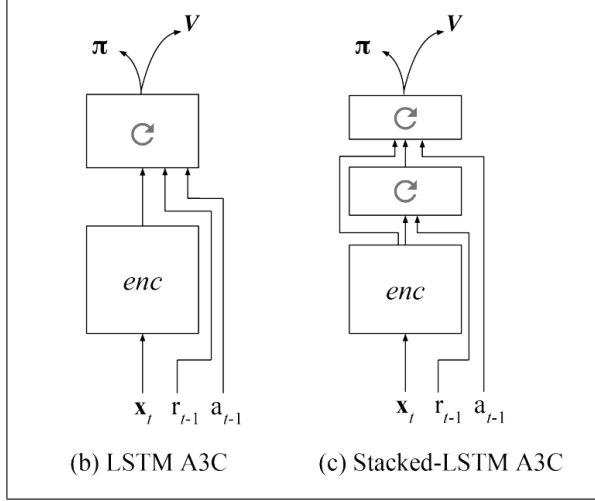


Fig. 8. Advantage actor-critic with recurrence. In all architectures, reward and last action are additional inputs to the LSTM. For non-bandit environments, observation is also fed into the LSTM either as a one-hot or passed through an encoder model [3-layer encoder: two convolutional layers (first layer: 16 8x8 filters applied with stride 4, second layer: 32 4x4 filters with stride 2) followed by a fully connected layer with 256 units and then a ReLU non-linearity. See for details Mirowski et al. (2016)]. For bandit experiments, current time step is also fed in as input.  $\pi$  = policy;  $v$  = value function. A3C is the distributed multi-threaded asynchronous version of the advantage actor-critic algorithm (Mnih et al., 2016); A2C is single threaded. (a) Architecture used in experiments 1-5. (b) Convolutional-LSTM architecture used in experiment 6. (c) Stacked LSTM architecture with convolutional encoder used in experiments 6 and 7 [64]

A notable characteristic of both previously described setups is that the learning rate of the nested RNN is chosen lower compared to the outer optimization loop, consequently preventing the agent from overfitting to a single task  $m$ , yet gathering knowledge from the entire MDP space  $M$  [12].

### B. L2L in the Context of Spiking Neural Networks

When applied to Networks of Spiking Neurons, the previously described framework of L2L offers a promising alternative to common approaches which embed a series of biologically implausible ingredients. One major biological implausibility in learning algorithms employing error feedback is suggested by evidence, that real neurons almost certainly lack weight transport when unrolling the chain rule of backpropagation on the backward pass[56] [13][15]. In order to calculate gradients of an error at the outputs of a network, these neurons would have to maintain information about the strength of synapses outside their local neighborhood, which

seems unrealistic from a biological point of view. This evidence suggests the existence of a more sophisticated system of learning signals, which don't require information on global synaptic weights. Furthermore, oversimplistic models of real neurons, such as the Leaky integrate-and-fire neuron, lack key characteristics of real neurons and are often even further modified by engaging derivative surrogate functions in order to deal with the non-differentiable nature of spiking neurons. Among these mismatches between biological neurons and their artificial models is the ability of biological neurons, to adapt to previously experienced inputs and weights [56]. The ability to adapt to previous spikes of presynaptic neurons however not merely represents a visual difference but can be interpreted as the ability to store temporal information.

By deploying adaptive LIF neurons in a Network of Spiking Neurons, Bellec et al.[6] were able to overcome not only a discrepancy between model and reality but also achieved a well working long short-term memory, thus creating a new type of Recurrent Network of Spiking Neurons, the LSNN. The adaptivity of neurons is here realized by increasing the firing threshold  $B_j(t)$  of a neuron  $j$  by a fixed amount  $\frac{\beta}{\tau_{a,j}}$  for incoming spike trains  $z_j(t)$  and decaying it exponentially to a baseline  $b_j^0$  value in spike-free intervals with time constant  $\tau_{a,j}$ . The time constant can be chosen to fit the desired range of the created short-term memory. For discrete timesteps of  $\delta t = 1ms$  the dynamics of the adaptive threshold becomes (18) with the recursive update rule (19):

$$B_j(t) = b_j^0 + \beta b_j(t) \quad (18)$$

$$b_j(t + \delta t) = e^{-\frac{\delta t}{\tau_{a,j}}} b_j(t) + (1 - e^{-\frac{\delta t}{\tau_{a,j}}}) z_j(t) \quad (19)$$

As pointed out in the meta-RL, a well-working short-term memory is crucial to the ability to store learned experience on different levels of abstraction and now allows for the application of L2L to a network of spiking neurons. On a side note, the increase of the firing threshold in the adaptive neurons clearly leads to an overall decrease of spikes, thus operating more energy efficiently when deployed on neuromorphic hardware. The network architecture comprises additional sets of non-adaptive excitatory and inhibitory LIF neurons [6](s. fig. x). Similarly to Wang et al.[64], the synaptic weights of this network are subject to optimization of an outer loop algorithm, in this case a combination of BPTT and a biologically inspired rewiring method called DEEP R [5](s. fig. x). Since BPTT requires calculation of error gradients, the authors utilized a pseudo-derivate to surrogate the non-existing derivative of neuronal spike trains which comprises a simple damped triangular function. The synaptic weights are updated only after completed runs of tasks, while in-task optimization is realized through internal memory dynamics according to (17) and (18). Further details on the network setup and implementation can be reviewed in [6].

These results of this model might already offer interesting perspectives from a biological and neuroscientific view, ability to learn on different levels of abstraction,

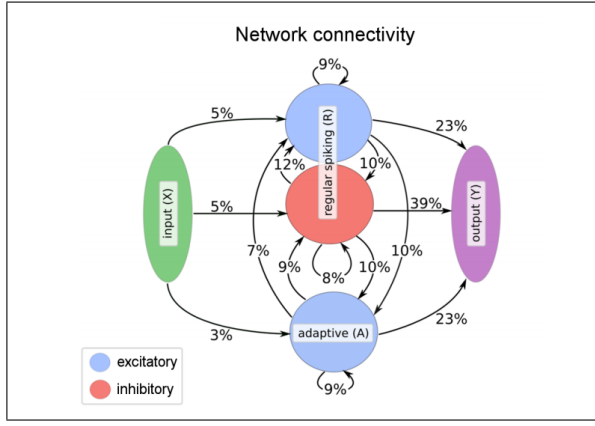


Fig. 9. Basic architecture of LSNN. Percentages on synaptic connections represent connectivity of the LSNN after applying DEEP R in conjunction with BPTT. Populations X,Y and R of regular spiking LIF neurons coupled with a population A of adaptive LIF neurons. [6]

so far a central asset biological brains. However one is tempted to wonder if this framework can be applied to more biologically plausible models on a technical level. Recall that the previously described setup including BPTT still requires the transport of global weight information as well as a transmission of error signals through time which are widely considered implausible in real RNNs. Bellec et al.[7] consequently developed an approach designed to tackle these shortcomings. The chapter "eligibility traces" already hinted at the possibility of avoiding the need for weight transport in credit assignment by conducting error propagation through dynamic eligibility traces. Bellec et al. take up the learning rule (17) with a different motivation, namely the approximation of error gradients. The fundamental role of eligibility traces in this algorithm led to the name e-Prop. The underlying basis for e-Prop is the assumption, that error gradients w.r.t. a synaptic weight  $\theta_{ji}$  can be factorized into a Learning signal  $L_j^t$  and its eligibility trace  $e_{ji}^t$ , summed up over time[7]:

$$\frac{dE}{d\theta_{ji}} = \sum_t L_j^t e_{ji}^t \quad (20)$$

Bellec et al.'s claim for biological plausibility is coupled to obtaining the learning signal  $L_j^t$  in a way, that does not require a propagation of error gradients through time or numerous layers (fig.x). In the following we will focus on two different approximations for these learning signals  $\hat{L}_{j1}^t$  and  $\hat{L}_{j2}^t$  constituting two versions e-Prop 1 and e-Prop 2.

E-Prop 1 uses the findings described in "feedback alignment" to broadcast error signals directly to the affected synaptic weights while adopting a random weight matrix instead of the actual weights. Assuming an error at the output layer  $k$  of leaky readout neurons  $y_k^t$  of  $((y_k^{*,t} - y_k^t))$  our Learning signal to a neuron  $\theta^{rec_{ji}}$  thus becomes  $\sum_k B^{random_{jk}}(y_k^{*,t} - y_k^t)$  instead of  $\sum_k \theta^{out_{kj}}(y_k^{*,t} - y_k^t)$ . Since this network is an RSNN, these learning signals are broadcasted to all synaptic weights in different time slices of

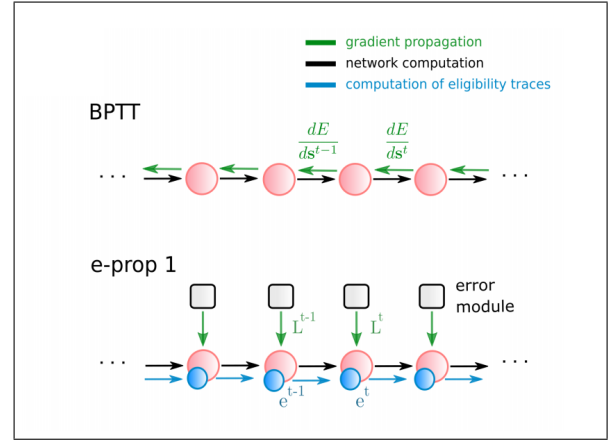


Fig. 10. Illustration of the error signal flow through network layers. Evidently, e-prop 1 does not require information transport in a backwards pass. (ill. from [7])

an unrolled recurrent network. The authors however reached better results when choosing the random weight projection matrix to be constant over all time-slices.

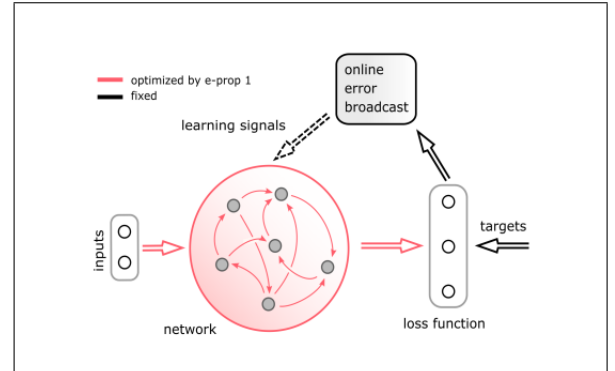


Fig. 11. Basic architecture of e-prop 1. Error broadcasts are calculated online at the output layer and sent directly to deeper layers of the RSNN, avoiding the necessity for weight transport on the backwards pass.(ill. from [7])

This approach is applicable to architectures with short-term memory, such as LSNNs, thus providing a basis for L2L frameworks, where learning on different levels could be allocated to the outer optimization through e-prop 1 and inner adaptive memory variables.

However Bellec et al. developed a second version of e-Prop, specifically dedicated to the utilization of L2L, called e-Prop 2. Neuroscience has long considered the existence of a sophisticated system of error feedback generation, where a sudden sharp negative potential in the brain called error-related negativity (ERN) is suspected to play a role in reflecting such error signals. ERN accompanies motoric misbehaviour responses and typically peaks within 80ms - 120ms after beginning of an error signal [23][19]. However further research remarkably points out that ERN can be observed even before motoric feedback becomes evident through sensory feedback, implying the existence of additional error response- and prediction systems embedded in biological neural networks [43] which may well be

a result of evolutionary development. Motivated by this finding, Bellec et al.[7] engaged an additional RSNN solely designed to generate optimized learning signals in e-Prop 2's architecture. These error-modules now take over the role of an outer-loop meta learner as mentioned in the chapter "meta-RL". Learning of the error module is again accomplished by training on a whole family of tasks  $F$  with BPTT. Conceivably, the application of BPTT contradicts the claim for biological plausability, howbeit the authors argue that the origin of well-developed systems of error-prediction and signal-generation are not fully understood but do not require biologically plausible optimization algorithms if interpreted as priors formed by a long process of evolution. The error module contains weights  $\Psi$  and receives the inputs  $\mathbf{x}^t$  and a target vector  $m\mathbf{y}^{*,t}$  which may be the target output of the network or a desired target state (e.g. a target vector may be the position of a robotic manipulator at time  $t$ , while the network output are joint velocities) [7]. A distinct difference between this setup and meta-RL or L2L LSNNs lies within the split network neurons of outer meta-learner and inner learner. Since the outer error modules now possess their own set of neurons with weights  $\Psi$ , the inner learner can store learned experience in its own set of synaptic weights  $\theta$ , implicitly alleviating the categorical need for short-term memory.

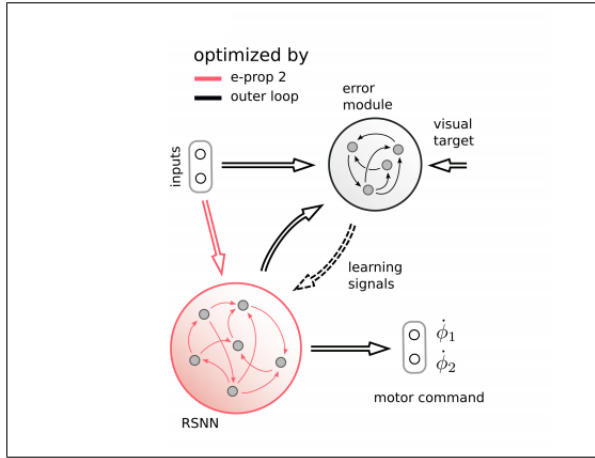


Fig. 12. Basic architecture of e-prop 2. An Error module network receives network inputs, a target state and the network state to produce learning signals optimized to improve learning in a nested RSNN (ill. [7]).

Training of this model is split into a training phase and a testing phase both consisting of exactly one trial. The initial output of the inner learner considering a specific task  $C$  therefore depends on its initial set of weights  $\theta_{\text{init}}$ . As e-Prop 2 optimizes  $\theta_{\text{init}}$  after a single training trial using its own initial weights  $\Psi_{\text{init}}$ , the output on the test trial with the same specific task  $C$  is now a result of the improved priors  $\theta_{\text{test},C}$ . A cost function for BPTT in the error module is created from the results of the test run  $L_C(\theta_{\text{test},C})$ . The complete learning dynamics of e-Prop 2 are then described by the minimization problem (21) and the update rule (22):

$$\min\{\mathbf{E}_{C \sim \mathcal{F}}[L_C(\theta_{\text{test},C})]\} \quad (21)$$

$$(\theta_{\text{test},C})_{ji} = (\theta_{\text{init}})_{ji} - \eta \sum_t \hat{L}_j^t e_{ji}^t \quad (22)$$

Duan et al.[20] identified the outer-loop optimization algorithm as an imminent bottleneck to this approach, hence it comes as little surprise, that further approaches such as the work by Bohnstingl et al.[9] have aimed at designing better outer-loop algorithms. The unsolved status of L2L architectures inspired the authors to implement a modular setup in which the optimization algorithms for the outer loop as well as the inner learner can easily be exchanged, allowing a fast evaluation of various possible algorithms. In particular, gradient-free optimization algorithms were employed to generate well-performing hyperparameters of a learner concerning a family of tasks. Here, Cross-Entropy (CE) [11], Evolution Strategies(ES) [8] and Simulated Annealing(SA)[37] were applied to mimic evolutionary processes involved in the development of human learning. CE and ES are metaheuristic global optimization algorithms designed to regions of well-performing parameters, while SA generates a single set of parameters. Given their probabilistic nature, these algorithms tend to be computationally expensive and were thus deployed to neuromorphic hardware to ensure feasibility [9]. In comparison to e-Prop, Bohnstingl et al. arranged a setup in which a new learning rule itself is represented by a multilayer perceptron (MLP) ANN and fitted by adjusting its weights and biases (fig. x).

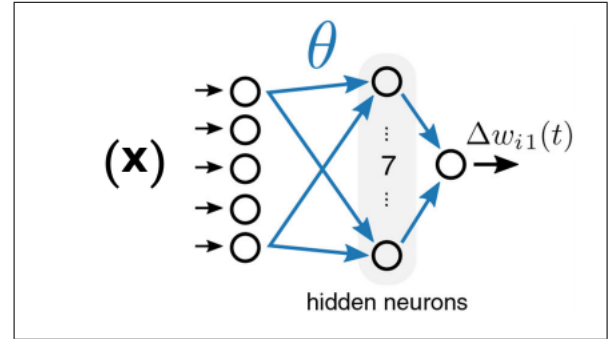


Fig. 13. MLP architecture of meta-plasticity with inputs  $(\mathbf{x})$ , one hidden layer of seven neurons and parameters  $\theta$ . The network outputs the weight updates for the agent-network. (ill. edited from [9]).

The resulting learning rule  $f_{ANN}(\mathbf{x}_{ji}(t); \theta)$  is called meta-plasticity and offers a new perspective on how synaptic plasticity in SNNs may be adjusted to boost performance on whole task families. Meat-plasticity, polished over various tasks of a family  $F$ , may enable an SNN-based learner to better perform on each of these tasks by adhering to the simple weight update (23):

$$\Delta w_{ji} = f_{ANN}(\mathbf{x}_{ji}(t); \theta) \quad (23)$$

Bohnstingl et al. conclude, that the algorithm applied in the outer loop of an L2L framework is crucial to its function and emphasize the stability offered by CE and ES due the generation of regions of well-working parameters as opposed to single values in SA. The perspective of declaring even plasticity rules subject to L2L optimization might offer new



paths for research and eventually provide important insights into learning in biological networks of neurons.

## V. APPLICATIONS OF L2L IN ROBOTICS

Robotics has undergone many successful developments in the recent past with advances being pushed from numerous fields of engineering, including that of machine learning. Yet the design process is still a tedious and highly tailored one, requiring many domain experts. Many of the underlying algorithms in the control, motion planning and sensoric interpretation require suitable setups of the environment with little room for variation. For example industrial manipulator robots can perform outstandingly when placed in a fixed production line, yet recognizing and grasping everyday objects in a kitchen or workshop poses a much higher challenge, as it requires the skill to make sense of broad environments with numerous imaginable tasks. Furthermore the dominating problems of applying RL in robotics can be summarized by the following problem classes [55]:

- Sample efficiency
- Sim2Real
- Reward function optimization
- Safety

The previous sections revealed a high potential in L2L frameworks in terms of sample efficiency and generalization, thus constituting feasible answers to expensive data generation or overfitting to simulator-specific features. However this further implies a reflection on the scalability of said L2L approaches in order to evaluate their applicability in the often very high-dimensional task spaces faced in robotics.

Wang et al.[64] examine meta-RL's ability to detect abstract task structures in large scale problems by adapting a well-known behavioural experiment described by Harlow [32] to a visual fixation task. In Harlows experiment, monkeys were presented two unfamiliar objects, with one hiding a bowl filled with food and while the other holds an empty bowl. The monkeys were allowed to choose one of the objects and received the reward, if present. Despite switching the objects for new unknown objects in each episode, upon replaying several trials in several episodes of this game, the animals showed a general understanding of the underlying structure of the problem. After beginning a new episode with new objects, the monkeys would, inevitably, take one random guess but managed to succeed in the following trials of the episode [12].

### A. Tasks in high-dimensional spaces

Motion and path planning are fundamental problems in robotics, whether it be within a space of rich visual input, sensory data or configuration/joint-spaces. Similiar to the problem described by Harlow, the navigational task in the I-maze environment as described by Mirowski et al.[46] and Jaderberg et al.[36] requires an understanding of the general structure of the problem in order to learn sample-efficiently on the specific task. In this case the same maze spawns a

goal location on random position within the maze where the agent has to learn a motion path to the goal in as few trials as possible. The results of Wang et al.[64] show, that an architecture of stacked LSTM is able to solve the task after having conducted one exploration run (finishing the episode in 100 timesteps) notably faster ( 30 timesteps) within few explotation runs. The reference baseline, a feedforward architecture A3C learner, is not able to solve the problem at all.

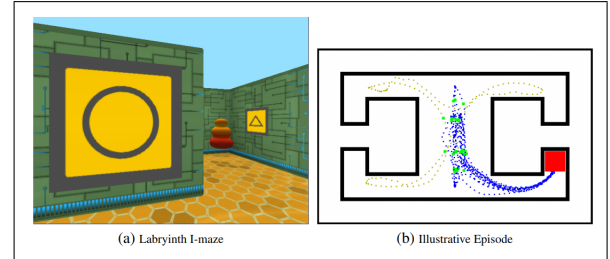


Fig. 14. a) view of I-maze showing goal object in one of the 4 alcoves b) following initial exploration (light trajectories), agent repeatedly goes to goal (blue trajectories) c) Performance of stacked LSTM (termed Nav A3C) and feedforward (FF A3C) architectures, per episode (goal = 10 points) averaged across top 5 hyperparameters. e) following initial goal discovery (goal hits marked in red), value function occurs well in advance of the agent seeing the goal which is hidden in an alcove. [64]

Duan et al.[22] take a similiar approach in their evaluation of the feasibility of RL in high-dimensional state spaces. Again a randomly generated maze with a randomly placed target is chosen as the problem to solve for the agent. During one test run, the agent is given a number of episodes during which the maze structure and target position remain fixed. In contrast to an earlier approach to this RL-Task shown by Oh et al. [51] RL bases its actions within a more granular action space. The environments sparse reward payout design (+1 for target, -0.001 for wall hits, -0.04 per time frame) poses additional challenges to the agents learning and requires well-developed exploration strategies in the first episode in order to gain information on the problems ground structure. Cross-validation with a small and a larger version of the maze environment show a significant reduction in solving trajectory lengths between the first to episodes and indicate, that the RL algorithm managed to utilize previously gained information to come to good solutions more quickly. However the shown results are not yet optimal as the agent still forgets, though rarely, initially explored target positions and explores further paths in the second episode. Duan et al. indicate that further improvements might come with improved RL-algorithms as the outer-loop optimizer (fig. x).

Bellec et al.[6] tested an implementation of LSNN on a navigational task in a 2D arena in reinforcement learning to demonstrate applicability in complex environments. The LSNN-based agent was palced in a circular arena in which a specific task  $M$  would be to reach a goal within this arena on a fixed position, while the whole family  $F$  of tasks would include various goal positions within this arena. By setting these goal positions to be close to the arena boundaries, the agent is challenged to develop an abstract

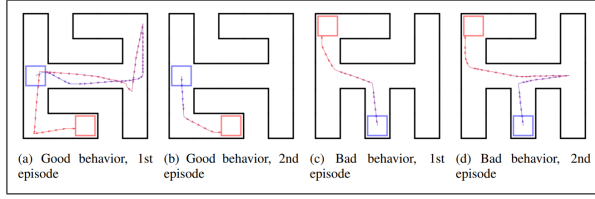


Fig. 15. Visualization of the agents behavior. In each scenario, the agent starts at the center of the blue block, and the goal is to reach anywhere in the red block [22].

understanding of the commonalities between all tasks, which he can exploit when facing one of the tasks  $M$ . For each of these specific tasks, the objective is to reach the goal (at a fixed position throughout one task  $M$ ) as many times as possible within a fixed time frame after being placed randomly upon reaching the goal. The according sparse reward function was chosen to award goal attainment with a score of 1 while hitting the arena boundaries will lead to -0.02 punishment. According to the applied L2L framework, outer-loop optimization through BPTT and DEEP-R was performed on the synaptic weights over the whole task family  $F$ , while specific task optimization was accomplished by adapting the short-term memory, i.e. the thresholds of the adaptive LIF neurons. Remarkably this model was able to generate an abstract understanding of the characteristic of the task, exhibiting human-like strategies to first explore the boundaries of the given environment to find the goal position and utilizing this knowledge to efficiently reach the goal in subsequent runs (fig. x).

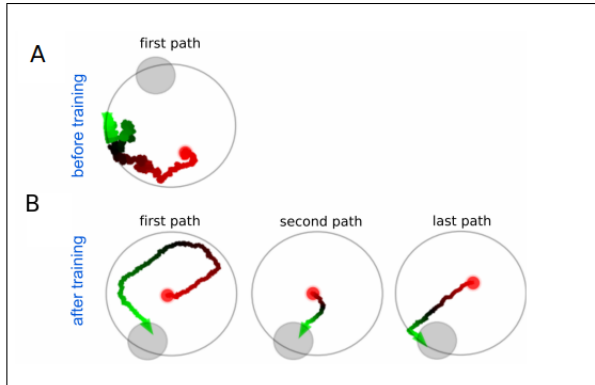


Fig. 16. **A:** The untrained model does not show any strategic or efficient way to find the goal. (Bellec et al.)

**B:** The trained model performs initial exploration runs alongside environment boundaries, exhibiting the abstract understanding that all tasks of family  $F$  share the characteristic of goals close to the arena boundaries. Efficient path-planning of the agent in the subsequent runs prove, that the adaptive LIF neurons were capable of storing the position of the goal in short-term memory. [6]

### B. Few-Shot Learning

One promising aspect of L2L is the capability of generalizing more than any conventional neural network. A model agile enough to understand underlying abstract knowledge about robotic motion does not only foreshadow better, more robust motoric control but especially a reduction in training

data. Bellec et al.[7] evaluated e-Prop 2 on a one-shot learning task, where a trajectory of a 2-joint robotic arm should be learned by the agent. That is, the error modules of e-Prop 2 had previously been trained sufficiently on a family of robotic kinematic tasks to generate fitting learning signals  $\hat{L}_j^t$  and RSNN priors  $\theta_{init}$ . The learning phase of the agent was restricted to a single training run to gain a strict evaluation on the capabilities of the L2L system. Interestingly, the agent was not given an inverse kinematic model, thus requiring the model to understand the space mismatch between the endeffector pose (network target) in euclidean space and the joint space (network output). A family of tasks  $F$  was generated with each task  $C$  representing a randomly generated target trajectory of the arm endeffector. The inner RSNN is a network composed of 400 recurrent LIF neurons which receives inputs  $\mathbf{x}_t$  and outputs the required joint velocities to influencing the endeffector pose. An outer loop error module, consisting of 300 LIF neurons was previously trained with the inputs  $\mathbf{x}_t$ , spiking activity of the RSNN  $\mathbf{z}^t$  and the target trajectory  $y^{*,t}$  in Euclidean space. The optimization was conducted with BPTT over batches of 200 different tasks to minimize expectation of the loss sum across the family of tasks.

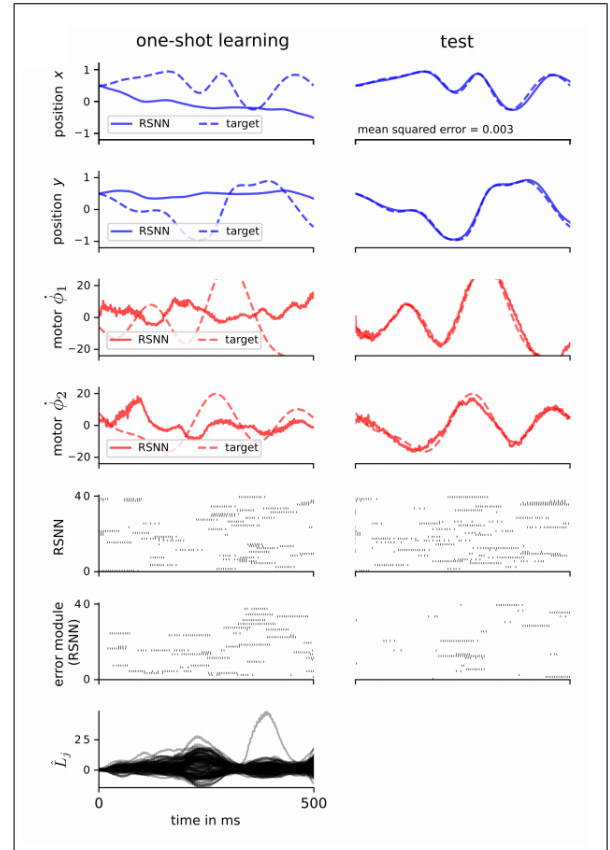


Fig. 17. Results of one-shot learning tasks before (left) and after (right) a single training trial. After a training run, the RSNN synaptic weights were updated using learning signal  $\hat{L}_j^t$  (bottom). In the fifth row, spikes in the error module have become sparse after the training run, which can be explained by the low error-rate generated by a learned RSNN [7]

Fig. x shows the result of the motor outputs by the RSNN

after a single training trial, provided the error modules experienced sufficient training. In plots 1-4 it becomes apparent, that the first and only training trial was inevitably unsuccessful but generally sufficed to generate trajectories with a MSE of 0.003 after a single update of weights with Learning signals from an outer error module. We can conclude, that the network has achieved one-shot learning capability for the infinitely large family of random trajectories in a 2-joint robotic arm.

## VI. DISCUSSION

The heretofore described framework of L2L and its various applications poses promising perspectives for future work in the fields of machine learning, robotics but also neuroscience and cognitive sciences. Historically, these fields have been intertwined and underwent phases of more and phases of less interaction but nonetheless generated implications that could be of scientific use for the other. Cognitive sciences provide ideas and inspirations for ever further sophisticated algorithms, while Artificial Neural Networks can offer evaluations of plausibility for biological models or in turn stimulate new implications for neuroscience on the basis of well-working algorithmic models. L2L is particularly interesting when considering the gap in learning efficiency between human brains and ANNs. The idea of certain preshaped priors inert to human brains is certainly not new to cognitive sciences and seem quite obvious when regarding how the uniform efficiency with which all human brains are capable of learning. However conclusions on the origin and development of such preengineered priors remain vague and manifold. Wang et al.[63] propose, that midbrain dopamine-driven synaptic plasticity in the brain may well be an outer-loop optimization system shaping learning in the prefrontal cortex (PFC), which in turn acts as a hierarchically lower learner. The dopamine neurons of the midbrain are thought to employ reward prediction error signals which shape synaptic connectivity in such a way that animals are prone to improve performance [48]. It is however up to debate, to which extent these signals contain information which is based on a environment-dependent model (model-based) or occur model-free. For example, [17]Daw et al. discovered evidence, that signals strongly correlated to dopaminergic prediction errors contain robust model-based information [12][17]. In this regard, Wang et al.[63] point out that a meta-RL system trained with a model-free RL algorithm can generate model-based like behaviour in the inner loop algorithm. They suggest that very similarly, human brains may actually operate in a grey area between model-free and model-based RL and do so in coordination with the uniformity of environmental structures.

Bellec et al.[6] yield a different interpretation of the nested nature of L2L and argue that sophisticated priors and learning algorithms have been shaped by long evolutionary processes. In fact this perspective alleviates the imminent need for biologically implausible processes such as the backpropagation of error-gradient learning signals through

multiple layers and even time. By optimizing directly broadcasted learning signals coupled with eligibility traces of spiking neurons, Bellec et al. were the first to reproduce meta-learning in networks of spiking neurons and provide promising results, albeit not yet surpassing performance of BPTT-based ANNs.

On another note, the implementation and performance of SNNs is strongly linked to the development of fitting neuromorphic hardware and appropriate algorithms. Taking into consideration the analogy of evolution for L2L, it should come with little surprise that the outer loop optimization of L2L is considered a crucial bottleneck in terms of capability and computational efforts [21]. In the light of energy and computation efficiency, LSNNs exhibit the remarkable characteristic of sparse firing activity and implies further capabilities in activity-silent memory, much like human brains.

Applications of L2L such as the experiments described in previous chapters point at the opportunities of this approach but to this date remain proof-of-concepts. Duan et al.[22] hold upscaling of L2L for broader distributions of tasks to be the most important next step in this approach. It is yet to be determined, how L2L models could be combined to generate a single system with dedicated learning modules to tackle applications which require vast ranges of skills. Large-scale projects such as the "Scalable Deep Reinforcement Learning for Robotic Manipulation" by Google Brain[1] are evidence of the imminent need for data efficient, generalizing learning algorithms, especially in the light of the immense efforts currently needed to apply deep learning algorithms in robotics. Simulation based projects like "Learning Dexterity" by OpenAI [3] are challenged by sim2real and again invest immense efforts in domain randomization approaches. A network architecture that promises greater generalization ability could hold answers for better results in terms of stability and safety as well. Especially when deployed in large machines (e.g. industrial robotics, autonomous driving), Deep Learning is required to adhere to high safety standards with nearly impossible-to-get training data. L2L might therefore be part of some of the largest upcoming challenges faced in this field.

## REFERENCES

- [1] Scalable Deep Reinforcement Learning for Robotic Manipulation.
- [2] Understanding LSTM Networks – colah’s blog. <http://colah.github.io/posts/2015-08-Understanding-LSTMs/>.
- [3] Learning Dexterity. <https://openai.com/blog/learning-dexterity/>, July 2018.
- [4] L. F Abbott. Lapique’s introduction of the integrate-and-fire model neuron (1907). *Brain Research Bulletin*, 50(5):303–304, November 1999.
- [5] Guillaume Bellec, David Kappel, Wolfgang Maass, and Robert Legenstein. Deep Rewiring: Training very sparse deep networks. *arXiv:1711.05136 [cs, stat]*, November 2017.
- [6] Guillaume Bellec, Darjan Salaj, Anand Subramoney, Robert Legenstein, and Wolfgang Maass. Long short-term memory and Learning-to-learn in networks of spiking neurons. In S. Bengio, H. Wallach, H. Larochelle, K. Grauman, N. Cesa-Bianchi, and R. Garnett, editors,

- Advances in Neural Information Processing Systems 31*, pages 787–797. Curran Associates, Inc., 2018.
- [7] Guillaume Bellec, Franz Scherr, Elias Hajek, Darjan Salaj, Robert Legenstein, and Wolfgang Maass. Biologically inspired alternatives to backpropagation through time for learning in recurrent neural nets. *arXiv:1901.09049 [cs]*, January 2019.
  - [8] Hans-Georg Beyer and Hans-Paul Schwefel. Evolution strategies - A comprehensive introduction. *Natural Computing*, 1:3–52, March 2002.
  - [9] Thomas Bohnstingl, Franz Scherr, Christian Pehle, Karlheinz Meier, and Wolfgang Maass. Neuromorphic Hardware Learns to Learn. *Frontiers in Neuroscience*, 13, May 2019.
  - [10] Sander M Bohte and Joost N Kok. SpikeProp: Backpropagation for Networks of Spiking Neurons. page 7.
  - [11] Zdravko I. Botev, Dirk P. Kroese, Reuven Y. Rubinstein, and Pierre L’Ecuyer. The Cross-Entropy Method for Optimization. In *Handbook of Statistics*, volume 31, pages 35–59. Elsevier, 2013.
  - [12] Matthew Botvinick, Sam Ritter, Jane X. Wang, Zeb Kurth-Nelson, Charles Blundell, and Demis Hassabis. Reinforcement Learning, Fast and Slow. *Trends in Cognitive Sciences*, 23(5):408–422, May 2019.
  - [13] Lakshminarayan V. Chinta and Douglas Blair Tweed. Adaptive Optimal Control Without Weight Transport. *Neural Computation*, 24:1487–1518, 2012.
  - [14] Kyunghyun Cho, Bart van Merriënboer, Caglar Gulcehre, Dzmitry Bahdanau, Fethi Bougares, Holger Schwenk, and Yoshua Bengio. Learning Phrase Representations using RNN Encoder-Decoder for Statistical Machine Translation. *arXiv:1406.1078 [cs, stat]*, June 2014.
  - [15] Francis Crick. The recent excitement about neural networks. *Nature*, 337(6203):129, January 1989.
  - [16] Yang Dan and Mu-Ming Poo. Spike timing-dependent plasticity: From synapse to perception. *Physiological Reviews*, 86(3):1033–1048, July 2006.
  - [17] Nathaniel D. Daw, Samuel J. Gershman, Ben Seymour, Peter Dayan, and Raymond J. Dolan. Model-based influences on humans’ choices and striatal prediction errors. *Neuron*, 69(6):1204–1215, March 2011.
  - [18] Gustavo Deco and Edmund T. Rolls. A Neurodynamical cortical model of visual attention and invariant object recognition. *Vision Research*, 44(6):621–642, March 2004.
  - [19] Ziya V. Dikman and John J. B. Allen. Error monitoring during reward and avoidance learning in high- and low-socialized individuals. *Psychophysiology*, 37(1):43–54, 2000.
  - [20] Yan Duan, Marcin Andrychowicz, Bradley Stadie, OpenAI Jonathan Ho, Jonas Schneider, Ilya Sutskever, Pieter Abbeel, and Wojciech Zaremba. One-Shot Imitation Learning. In I. Guyon, U. V. Luxburg, S. Bengio, H. Wallach, R. Fergus, S. Vishwanathan, and R. Garnett, editors, *Advances in Neural Information Processing Systems 30*, pages 1087–1098. Curran Associates, Inc., 2017.
  - [21] Yan Duan, Xi Chen, Rein Houthooft, John Schulman, and Pieter Abbeel. Benchmarking Deep Reinforcement Learning for Continuous Control. page 10.
  - [22] Yan Duan, John Schulman, Xi Chen, Peter L. Bartlett, Ilya Sutskever, and Pieter Abbeel. RL\$2\$: Fast Reinforcement Learning via Slow Reinforcement Learning. *arXiv:1611.02779 [cs, stat]*, November 2016.
  - [23] William J. Gehring, Brian Goss, Michael G. H. Coles, David E. Meyer, and Emanuel Donchin. The Error-Related Negativity. *Perspectives on Psychological Science*, 13(2):200–204, March 2018.
  - [24] F. A. Gers and J. Schmidhuber. Recurrent nets that time and count. In *Proceedings of the IEEE-INNS-ENNS International Joint Conference on Neural Networks. IJCNN 2000. Neural Computing: New Challenges and Perspectives for the New Millennium*, volume 3, pages 189–194 vol.3, July 2000.
  - [25] Wulfram Gerstner. Spike-response model. *Scholarpedia*, 3(12):1343, December 2008.
  - [26] Alex Graves. Adaptive Computation Time for Recurrent Neural Networks. *arXiv:1603.08983 [cs]*, March 2016.
  - [27] Alex Graves and Navdeep Jaitly. Towards End-to-End Speech Recognition with Recurrent Neural Networks. page 9.
  - [28] Alex Graves, Greg Wayne, and Ivo Danihelka. Neural Turing Machines. *arXiv:1410.5401 [cs]*, October 2014.
  - [29] Andre Gruning and Sander M Bohte. Spiking Neural Networks: Principles and Challenges. *Computational Intelligence*, page 10, 2014.
  - [30] Jiang Guo. BackPropagation Through Time. 2013.
  - [31] Moritz Hardt, Benjamin Recht, and Yoram Singer. Train faster, generalize better: Stability of stochastic gradient descent. *arXiv:1509.01240 [cs, math, stat]*, September 2015.
  - [32] Harry F. Harlow. The formation of learning sets. *Psychological Review*, 56(1):51–65, 1949.
  - [33] Sepp Hochreiter and Jürgen Schmidhuber. Long Short-Term Memory. *Neural Comput.*, 9(8):1735–1780, November 1997.
  - [34] A. L. Hodgkin and A. F. Huxley. A quantitative description of membrane current and its application to conduction and excitation in nerve. *The Journal of Physiology*, 117(4):500–544, August 1952.
  - [35] E. M. Izhikevich. Simple model of spiking neurons. *IEEE Transactions on Neural Networks*, 14(6):1569–1572, November 2003.
  - [36] Max Jaderberg, Volodymyr Mnih, Wojciech Marian Czarnecki, Tom Schaul, Joel Z. Leibo, David Silver, and Koray Kavukcuoglu. Reinforcement Learning with Unsupervised Auxiliary Tasks. *arXiv:1611.05397 [cs]*, November 2016.
  - [37] Scott Kirkpatrick, Charles Daniel Gelatt, and Mario P. Vecchi. Optimization by simulated annealing. *Science*, 220(4598):671–680, 1983.
  - [38] Benjamin James Lansdell and Konrad Paul Kording. Towards learning-to-learn. *arXiv:1811.00231 [cs, q-bio]*, November 2018.
  - [39] Robert Legenstein, Dejan Pecevski, and Wolfgang Maass. A Learning Theory for Reward-Modulated Spike-Timing-Dependent Plasticity with Application to Biofeedback. *PLoS computational biology*, 4:e1000180, November 2008.
  - [40] Wolfgang Maass. Networks of Spiking Neurons Learn to Learn and Remember. page 27.
  - [41] Wolfgang Maass. Networks of spiking neurons: The third generation of neural network models. *Neural Networks*, 10(9):1659–1671, December 1997.
  - [42] Dougal Maclaurin, David Duvenaud, and Ryan P Adams. Gradient-based Hyperparameter Optimization through Reversible Learning. page 10.
  - [43] Stephane J. MacLean, Cameron D. Hassall, Yoko Ishigami, Olav E. Krigolson, and Gail A. Eskes. Using brain potentials to understand prism adaptation: The error-related negativity and the P300. *Frontiers in Human Neuroscience*, 9:335, 2015.
  - [44] Nikola T. Markov, Julien Vezoli, Pascal Chameau, Arnaud Falchier, René Quilodran, Cyril Huisoud, Camille Lamy, Pierre Misery, Pascale Giroud, Shimon Ullman, Pascal Barone, Colette Dehay, Kenneth Knoblauch, and Henry Kennedy. Anatomy of hierarchy: Feedforward and feedback pathways in macaque visual cortex. *The Journal of Comparative Neurology*, 522(1):225–259, January 2014.
  - [45] Timothée Masquelier, Rudy Guyonneau, and Simon J. Thorpe. Spike timing dependent plasticity finds the start of repeating patterns in continuous spike trains. *PLoS One*, 3(1):e1377, January 2008.
  - [46] Piotr Mirowski, Razvan Pascanu, Fabio Viola, Hubert Soyer, Andrew J. Ballard, Andrea Banino, Misha Denil, Ross Goroshin, Laurent Sifre, Koray Kavukcuoglu, Dharshan Kumaran, and Raia Hadsell. Learning to Navigate in Complex Environments. *arXiv:1611.03673 [cs]*, November 2016.
  - [47] Volodymyr Mnih, Adrià Puigdomènech Badia, Mehdi Mirza, Alex Graves, Timothy P. Lillicrap, Tim Harley, David Silver, and Koray Kavukcuoglu. Asynchronous Methods for Deep Reinforcement Learning. *arXiv:1602.01783 [cs]*, February 2016.
  - [48] P. R. Montague, P. Dayan, and T. J. Sejnowski. A framework for mesencephalic dopamine systems based on predictive Hebbian learning. *Journal of Neuroscience*, 16(5):1936–1947, March 1996.
  - [49] Arvind Neelakantan, Jeevan Shankar, Alexandre Passos, and Andrew McCallum. Efficient Non-parametric Estimation of Multiple Embeddings per Word in Vector Space. *arXiv:1504.06654 [cs, stat]*, April 2015.
  - [50] Emre O. Neftci, Hesham Mostafa, and Friedemann Zenke. Surrogate Gradient Learning in Spiking Neural Networks. *arXiv:1901.09948 [cs, q-bio]*, January 2019.
  - [51] Junhyuk Oh, Satinder Singh, Honglak Lee, and Pushmeet Kohli. Zero-Shot Task Generalization with Multi-Task Deep Reinforcement Learning. *arXiv:1706.05064 [cs]*, June 2017.
  - [52] Wei-Xing Pan, Robert Schmidt, Jeffery R. Wickens, and Brian I. Hyland. Dopamine Cells Respond to Predicted Events during Classical Conditioning: Evidence for Eligibility Traces in the Reward-Learning Network. *Journal of Neuroscience*, 25(26):6235–6242, June 2005.
  - [53] Michael Pfeiffer and Thomas Pfeil. Deep Learning With Spiking Neurons: Opportunities and Challenges. *Frontiers in Neuroscience*, 12, October 2018.
  - [54] Filip Ponulak and Andrzej Kasiński. *Introduction to Spiking Neural Networks: Information Processing, Learning and Applications*, volume 71. January 2011.

- [55] Or Rivlin. Reinforcement Learning for Real-World Robotics. <https://towardsdatascience.com/reinforcement-learning-for-real-world-robotics-148c81dbdcff>, May 2019.
- [56] Arash Samadi, Timothy P. Lillicrap, and Douglas B. Tweed. Deep Learning with Dynamic Spiking Neurons and Fixed Feedback Weights. *Neural Computation*, 29(3):578–602, March 2017.
- [57] John Schulman, Sergey Levine, Philipp Moritz, Michael I. Jordan, and Pieter Abbeel. Trust Region Policy Optimization. *arXiv:1502.05477 [cs]*, February 2015.
- [58] M. Schuster and K. K. Paliwal. Bidirectional recurrent neural networks. *IEEE Transactions on Signal Processing*, 45(11):2673–2681, November 1997.
- [59] H. Sebastian Seung. Learning in Spiking Neural Networks by Reinforcement of Stochastic Synaptic Transmission. *Neuron*, 40(6):1063–1073, December 2003.
- [60] David Silver, Aja Huang, Chris J. Maddison, Arthur Guez, Laurent Sifre, George van den Driessche, Julian Schrittwieser, Ioannis Antonoglou, Veda Panneershelvam, Marc Lanctot, Sander Dieleman, Dominik Grewe, John Nham, Nal Kalchbrenner, Ilya Sutskever, Timothy Lillicrap, Madeleine Leach, Koray Kavukcuoglu, Thore Graepel, and Demis Hassabis. Mastering the game of Go with deep neural networks and tree search. *Nature*, 529(7587):484–489, January 2016.
- [61] Amirhossein Tavanaei, Masoud Ghodrati, Saeed Reza Kheradpisheh, Timothée Masquelier, and Anthony Maida. Deep learning in spiking neural networks. *Neural Networks*, 111:47–63, March 2019.
- [62] A. Waibel, T. Hanazawa, G. Hinton, K. Shikano, and K. J. Lang. Phoneme recognition using time-delay neural networks. *IEEE Transactions on Acoustics, Speech, and Signal Processing*, 37(3):328–339, March 1989.
- [63] Jane X. Wang, Zeb Kurth-Nelson, Dharshan Kumaran, Dhruva Tirumala, Hubert Soyer, Joel Z. Leibo, Demis Hassabis, and Matthew Botvinick. Prefrontal cortex as a meta-reinforcement learning system. *Nature Neuroscience*, 21(6):860–868, June 2018.
- [64] Jane X. Wang, Zeb Kurth-Nelson, Dhruva Tirumala, Hubert Soyer, Joel Z. Leibo, Remi Munos, Charles Blundell, Dharshan Kumaran, and Matt Botvinick. Learning to reinforcement learn. *arXiv:1611.05763 [cs, stat]*, November 2016.
- [65] P. J. Werbos. Backpropagation through time: What it does and how to do it. *Proceedings of the IEEE*, 78(10):1550–1560, October 1990.